

World Journal of *Clinical Cases*

World J Clin Cases 2021 June 26; 9(18): 4460-4880



OPINION REVIEW

- 4460 Surgery for pancreatic tumors in the midst of COVID-19 pandemic

Kato H, Asano Y, Arakawa S, Ito M, Kawabe N, Shimura M, Hayashi C, Ochi T, Yasuoka H, Higashiguchi T, Kondo Y, Nagata H, Horiguchi A

REVIEW

- 4467 Roles of exosomes in diagnosis and treatment of colorectal cancer

Umwali Y, Yue CB, Gabriel ANA, Zhang Y, Zhang X

MINIREVIEWS

- 4480 Dynamics of host immune responses to SARS-CoV-2

Taherkhani R, Taherkhani S, Farshadpour F

- 4491 Current treatment for hepatitis C virus/human immunodeficiency virus coinfection in adults

Laiwatthanapaisan R, Sirinawasatien A

- 4500 Anti-tumor effect of statin on pancreatic adenocarcinoma: From concept to precision medicine

Huang CT, Liang YJ

- 4506 Roles of vitamin A in the regulation of fatty acid synthesis

Yang FC, Xu F, Wang TN, Chen GX

ORIGINAL ARTICLE**Basic Study**

- 4520 Identification of the circRNA-miRNA-mRNA regulatory network and its prognostic effect in colorectal cancer

Yin TF, Zhao DY, Zhou YC, Wang QQ, Yao SK

- 4542 Tetramethylpyrazine inhibits proliferation of colon cancer cells *in vitro*

Li H, Hou YX, Yang Y, He QQ, Gao TH, Zhao XF, Huo ZB, Chen SB, Liu DX

Case Control Study

- 4553 Significance of highly phosphorylated insulin-like growth factor binding protein-1 and cervical length for prediction of preterm delivery in twin pregnancies

Lan RH, Song J, Gong HM, Yang Y, Yang H, Zheng LM

Retrospective Cohort Study

- 4559** Expected outcomes and patients' selection before chemoembolization—"Six-and-Twelve or Pre-TACE-Predict" scores may help clinicians: Real-life French cohorts results
Adhoute X, Larrey E, Anty R, Chevallier P, Penaranda G, Tran A, Bronowicki JP, Raoul JL, Castellani P, Perrier H, Bayle O, Monnet O, Pol B, Bourliere M

Retrospective Study

- 4573** Application of intelligent algorithms in Down syndrome screening during second trimester pregnancy
Zhang HG, Jiang YT, Dai SD, Li L, Hu XN, Liu RZ
- 4585** Evaluation of a five-gene signature associated with stromal infiltration for diffuse large B-cell lymphoma
Nan YY, Zhang WJ, Huang DH, Li QY, Shi Y, Yang T, Liang XP, Xiao CY, Guo BL, Xiang Y
- 4599** Efficacy of combination of localized closure, ethacridine lactate dressing, and phototherapy in treatment of severe extravasation injuries: A case series
Lu YX, Wu Y, Liang PF, Wu RC, Tian LY, Mo HY
- 4607** Observation and measurement of applied anatomical features for thoracic intervertebral foramen puncture on computed tomography images
Wang R, Sun WW, Han Y, Fan XX, Pan XQ, Wang SC, Lu LJ
- 4617** Histological transformation of non-small cell lung cancer: Clinical analysis of nine cases
Jin CB, Yang L
- 4627** Diagnostic value of amygdala volume on structural magnetic resonance imaging in Alzheimer's disease
Wang DW, Ding SL, Bian XL, Zhou SY, Yang H, Wang P
- 4637** Comparison of ocular axis and corneal diameter between entropion and non-entropion eyes in children with congenital glaucoma
Wang Y, Hou ZJ, Wang HZ, Hu M, Li YX, Zhang Z

Observational Study

- 4644** Risk factors for postoperative delayed gastric emptying in ovarian cancer treated with cytoreductive surgery and hyperthermic intraperitoneal chemotherapy
Cui GX, Wang ZJ, Zhao J, Gong P, Zhao SH, Wang XX, Bai WP, Li Y
- 4654** Clinical characteristics, gastrointestinal manifestations and outcomes of COVID-19 patients in Iran; does the location matters?
Mokarram P, Dalivand MM, Pizuorno A, Aligolighasemabadi F, Sadeghdoust M, Sadeghdoust E, Aduli F, Oskrochi G, Brim H, Ashktorab H
- 4668** AWGS2019 vs EWGSOP2 for diagnosing sarcopenia to predict long-term prognosis in Chinese patients with gastric cancer after radical gastrectomy
Wu WY, Dong JJ, Huang XC, Chen ZJ, Chen XL, Dong QT, Bai YY

Prospective Study

- 4681** Clinical outcomes and 5-year follow-up results of keratosis pilaris treated by a high concentration of glycolic acid

Tian Y, Li XX, Zhang JJ, Yun Q, Zhang S, Yu JY, Feng XJ, Xia AT, Kang Y, Huang F, Wan F

Randomized Controlled Trial

- 4690** Tenofovir disoproxil fumarate in Chinese chronic hepatitis B patients: Results of a multicenter, double-blind, double-dummy, clinical trial at 96 weeks

Chen XF, Fan YN, Si CW, Yu YY, Shang J, Yu ZJ, Mao Q, Xie Q, Zhao W, Li J, Gao ZL, Wu SM, Tang H, Cheng J, Chen XY, Zhang WH, Wang H, Xu ZN, Wang L, Dai J, Xu JH

SYSTEMATIC REVIEWS

- 4700** Mesenteric ischemia in COVID-19 patients: A review of current literature

Kerawala AA, Das B, Solangi A

- 4709** Role of theories in school-based diabetes care interventions: A critical review

An RP, Li DY, Xiang XL

CASE REPORT

- 4721** Alport syndrome combined with lupus nephritis in a Chinese family: A case report

Liu HF, Li Q, Peng YQ

- 4728** Botulinum toxin injection for Cockayne syndrome with muscle spasticity over bilateral lower limbs: A case report

Hsu LC, Chiang PY, Lin WP, Guo YH, Hsieh PC, Kuan TS, Lien WC, Lin YC

- 4734** Meigs' syndrome caused by granulosa cell tumor accompanied with intrathoracic lesions: A case report

Wu XJ, Xia HB, Jia BL, Yan GW, Luo W, Zhao Y, Luo XB

- 4741** Primary mesonephric adenocarcinoma of the fallopian tube: A case report

Xie C, Shen YM, Chen QH, Bian C

- 4748** Pancreas-preserving duodenectomy for treatment of a duodenal papillary tumor: A case report

Wu B, Chen SY, Li Y, He Y, Wang XX, Yang XJ

- 4754** Pheochromocytoma with abdominal aortic aneurysm presenting as recurrent dyspnea, hemoptysis, and hypotension: A case report

Zhao HY, Zhao YZ, Jia YM, Mei X, Guo SB

- 4760** Minimally invasive removal of a deep-positioned cannulated screw from the femoral neck: A case report

Yang ZH, Hou FS, Yin YS, Zhao L, Liang X

- 4765** Splenic Kaposi's sarcoma in a human immunodeficiency virus-negative patient: A case report

Zhao CJ, Ma GZ, Wang YJ, Wang JH

- 4772 Neonatal syringocystadenoma papilliferum: A case report
Jiang HJ, Zhang Z, Zhang L, Pu YJ, Zhou N, Shu H
- 4778 Disappeared intralenticular foreign body: A case report
Xue C, Chen Y, Gao YL, Zhang N, Wang Y
- 4783 Femoral neck stress fractures after trampoline exercise: A case report
Nam DC, Hwang SC, Lee EC, Song MG, Yoo JI
- 4789 Collision carcinoma of the rectum involving neuroendocrine carcinoma and adenocarcinoma: A case report
Zhao X, Zhang G, Li CH
- 4797 Therapeutic effect of autologous concentrated growth factor on lower-extremity chronic refractory wounds: A case report
Liu P, Liu Y, Ke CN, Li WS, Liu YM, Xu S
- 4803 Cutaneous myiasis with eosinophilic pleural effusion: A case report
Fan T, Zhang Y, Lv Y, Chang J, Bauer BA, Yang J, Wang CW
- 4810 Severe hematuria due to vesical varices in a patient with portal hypertension: A case report
Wei ZJ, Zhu X, Yu HT, Liang ZJ, Gou X, Chen Y
- 4817 Rare coexistence of multiple manifestations secondary to thalamic hemorrhage: A case report
Yu QW, Ye TF, Qian WJ
- 4823 Anderson-Fabry disease presenting with atrial fibrillation as earlier sign in a young patient: A case report
Kim H, Kang MG, Park HW, Park JR, Hwang JY, Kim K
- 4829 Long-term response to avelumab and management of oligoprogression in Merkel cell carcinoma: A case report
Leão I, Marinho J, Costa T
- 4837 Central pontine myelinolysis mimicking glioma in diabetes: A case report
Shi XY, Cai MT, Shen H, Zhang JX
- 4844 Microscopic transduodenal excision of an ampullary adenoma: A case report and review of the literature
Zheng X, Sun QJ, Zhou B, Jin M, Yan S
- 4852 Growth hormone cocktail improves hepatopulmonary syndrome secondary to hypopituitarism: A case report
Ji W, Nie M, Mao JF, Zhang HB, Wang X, Wu XY
- 4859 Low symptomatic COVID-19 in an elderly patient with follicular lymphoma treated with rituximab-based immunotherapy: A case report
Łącki S, Wyżgolik K, Nicze M, Georgiew-Nadziakiewicz S, Chudek J, Wdowiak K

- 4866** Adult rhabdomyosarcoma originating in the temporal muscle, invading the skull and meninges: A case report
Wang GH, Shen HP, Chu ZM, Shen J
- 4873** *Listeria monocytogenes* bacteremia in a centenarian and pathogen traceability: A case report
Zhang ZY, Zhang XA, Chen Q, Wang JY, Li Y, Wei ZY, Wang ZC

ABOUT COVER

Editorial Board Member of *World Journal of Clinical Cases*, Shingo Tsujinaka, MD, PhD, Assistant Professor, Senior Lecturer, Surgeon, Department of Surgery, Saitama Medical Center, Jichi Medical University, Saitama 330-8503, Japan. tsujinakas@omiya.jichi.ac.jp

AIMS AND SCOPE

The primary aim of *World Journal of Clinical Cases (WJCC, World J Clin Cases)* is to provide scholars and readers from various fields of clinical medicine with a platform to publish high-quality clinical research articles and communicate their research findings online.

WJCC mainly publishes articles reporting research results and findings obtained in the field of clinical medicine and covering a wide range of topics, including case control studies, retrospective cohort studies, retrospective studies, clinical trials studies, observational studies, prospective studies, randomized controlled trials, randomized clinical trials, systematic reviews, meta-analysis, and case reports.

INDEXING/ABSTRACTING

The *WJCC* is now indexed in Science Citation Index Expanded (also known as SciSearch®), Journal Citation Reports/Science Edition, Scopus, PubMed, and PubMed Central. The 2020 Edition of Journal Citation Reports® cites the 2019 impact factor (IF) for *WJCC* as 1.013; IF without journal self cites: 0.991; Ranking: 120 among 165 journals in medicine, general and internal; and Quartile category: Q3. The *WJCC*'s CiteScore for 2019 is 0.3 and Scopus CiteScore rank 2019: General Medicine is 394/529.

RESPONSIBLE EDITORS FOR THIS ISSUE

Production Editor: Ji-Hong Lin; Production Department Director: Xiang Li; Editorial Office Director: Jin-Lai Wang.

NAME OF JOURNAL

World Journal of Clinical Cases

ISSN

ISSN 2307-8960 (online)

LAUNCH DATE

April 16, 2013

FREQUENCY

Thrice Monthly

EDITORS-IN-CHIEF

Dennis A Bloomfield, Sandro Vento, Bao-Gan Peng

EDITORIAL BOARD MEMBERS

<https://www.wjgnet.com/2307-8960/editorialboard.htm>

PUBLICATION DATE

June 26, 2021

COPYRIGHT

© 2021 Baishideng Publishing Group Inc

INSTRUCTIONS TO AUTHORS

<https://www.wjgnet.com/bpg/gerinfo/204>

GUIDELINES FOR ETHICS DOCUMENTS

<https://www.wjgnet.com/bpg/GerInfo/287>

GUIDELINES FOR NON-NATIVE SPEAKERS OF ENGLISH

<https://www.wjgnet.com/bpg/gerinfo/240>

PUBLICATION ETHICS

<https://www.wjgnet.com/bpg/GerInfo/288>

PUBLICATION MISCONDUCT

<https://www.wjgnet.com/bpg/gerinfo/208>

ARTICLE PROCESSING CHARGE

<https://www.wjgnet.com/bpg/gerinfo/242>

STEPS FOR SUBMITTING MANUSCRIPTS

<https://www.wjgnet.com/bpg/GerInfo/239>

ONLINE SUBMISSION

<https://www.f6publishing.com>

Retrospective Study

Observation and measurement of applied anatomical features for thoracic intervertebral foramen puncture on computed tomography images

Ran Wang, Wei-Wei Sun, Ying Han, Xiao-Xue Fan, Xue-Qin Pan, Shi-Chong Wang, Li-Juan Lu

ORCID number: Ran Wang 0000-0001-8657-108X; Wei-Wei Sun 0000-0002-0814-942X; Ying Han 0000-0001-7894-1802; Xiao-Xue Fan 0000-0002-7253-1615; Xue-Qin Pan 0000-0003-1326-258X; Shi-Chong Wang 0000-0002-0612-3197; Li-Juan Lu 0000-0002-6571-8529.

Author contributions: Lu LJ and Wang R initiated and designed the experiments; Han Y, Fan XX, Pan XQ, and Wang SC completed the computed tomography image processing and characteristic measurement; Sun WW and Wang R completed the statistical work and wrote the article; Lu LJ revised the article; Wang R and Sun WW contributed equally to this work.

Supported by The Key R & D Project in Jiangsu Province, No. BE2017603 and No. BE2017675; and the Key Program of Medical Science and Technology Development Projects in Nanjing, No. ZKX19016.

Institutional review board

statement: This study was reviewed and approved by the Ethics Committee of Nanjing Drum Tower Hospital Clinical College of Xuzhou Medical University (2020-347-01).

Ran Wang, Wei-Wei Sun, Xue-Qin Pan, Li-Juan Lu, Department of Pain Management, Nanjing Drum Tower Hospital, Clinical College of Xuzhou Medical University, Nanjing 210008, Jiangsu Province, China

Ying Han, Xiao-Xue Fan, Shi-Chong Wang, Department of Pain Management, Nanjing Drum Tower Hospital, The Affiliated Hospital of Nanjing University Medical School, Nanjing 210008, Jiangsu Province, China

Corresponding author: Li-Juan Lu, MD, Chief Doctor, Department of Pain Management, Nanjing Drum Tower Hospital, Clinical College of Xuzhou Medical University, No. 321 Zhongshan Road, Nanjing 210008, Jiangsu Province, China. lulijuan@njgly.com

Abstract

BACKGROUND

Thoracic intervertebral foramen puncture is the key step for interventional therapy on the thoracic nerve roots or dorsal root ganglia. The anatomical features of the thoracic spine are complex, and puncture injury to the pleura, blood vessels, spinal cord, and other tissues may cause serious complications. The spatial anatomical characteristics and related parameters for thoracic intervertebral foramen puncture remain poorly understood.

AIM

To observe and summarize the spatially applied anatomical characteristics for intervertebral foramen puncture on different vertebral segments.

METHODS

A total of 88 patients (41 males and 47 females) who underwent thoracic minimally invasive interventional treatment at Nanjing Drum Tower Hospital from January 2019 to June 2020 were included. Computed tomography images of 167 thoracic vertebral segments scanned in the prone position were collected. The width of the intertransverse space (D_p), the height of the rib neck/head above the lower transverse process (D_r), the width of the lateral border of the articular process/lamina (W_p), and the width of the posterior border of the vertebral body (W_v) were measured. At the upper 1/3 of the intervertebral foramina, the horizontal inclination angle (α) from the lateral border of the articular process/lamina to the posterolateral border of the vertebral body was measured.

Informed consent statement:

Patients were not required to give informed consent to the study because the analysis used anonymous clinical image data from picture archiving and communication system. Non-informed consent has been allied to the Ethics Committee of Nanjing Drum Tower Hospital Clinical College of Xuzhou Medical University.

Conflict-of-interest statement: All authors have nothing to disclose.

Data sharing statement: No additional data are available.

Open-Access: This article is an open-access article that was selected by an in-house editor and fully peer-reviewed by external reviewers. It is distributed in accordance with the Creative Commons Attribution NonCommercial (CC BY-NC 4.0) license, which permits others to distribute, remix, adapt, build upon this work non-commercially, and license their derivative works on different terms, provided the original work is properly cited and the use is non-commercial. See: <http://creativecommons.org/licenses/by-nc/4.0/>

Manuscript source: Unsolicited manuscript

Specialty type: Anatomy and morphology

Country/Territory of origin: China

Peer-review report's scientific quality classification

Grade A (Excellent): 0
Grade B (Very good): B
Grade C (Good): 0
Grade D (Fair): 0
Grade E (Poor): 0

Received: January 19, 2021

Peer-review started: January 19, 2021

First decision: March 25, 2021

Revised: April 5, 2021

Accepted: April 20, 2021

Article in press: April 20, 2021

Published online: June 26, 2021

The ratios D_R/D_P and W_P/W_V were calculated. The intervertebral foramen parameters were compared between segments.

RESULTS

No rib head/neck occlusion ($D_R/D_P > 0$) was found in the intertransverse spaces of T1-2 and T12-L1. The incidence of occlusion for the upper thoracic segments (T1-5, $n = 138$), middle thoracic segments (T5-9, $n = 116$), and lower thoracic segments (T9-L1, $n = 80$) were 76.81%, 100%, and 82.50%, respectively. The incidence of occlusion for the middle thoracic segments was significantly higher than that for the upper and lower thoracic segments ($P < 0.05$). The incidence of $> 1/2$ occlusion ($D_R/D_P > 1/2$) for the upper, middle, and lower thoracic segments was 7.97%, 74.14%, and 32.50%, respectively. The incidence of $> 1/2$ occlusion for the middle thoracic segments was significantly higher than that for the upper and lower thoracic segments ($P < 0.05$). W_P was longer than W_V on T1-2 to T9-10 and shorter than W_V on T10-11 to T12-L1. The horizontal puncture angle (α) into the external opening of the intervertebral foramina was positively correlated with the segments of the thoracic vertebrae from the cephalic to caudal portion (left: $r = 0.772$, $P < 0.01$; right: $r = 0.771$, $P < 0.01$), and the horizontal inclination angle for T11-12 and T12-L1 was 90° .

CONCLUSION

It is necessary to identify the spatial impact of the rib head/neck on the puncture path of the intervertebral foramina and design appropriate puncture angles for different segments.

Key Words: Thoracic intervertebral foramen; Puncture; Computed tomography; Three-dimensional reconstruction; Rib

©The Author(s) 2021. Published by Baishideng Publishing Group Inc. All rights reserved.

Core Tip: We measured and summarized the features of applied anatomy for thoracic intervertebral foramina cannulation. Based on our results, we found that the rib head/neck in the middle thoracic segments greatly influences the puncture path for the intervertebral foramen. It is necessary to identify the space between the transverse process and rib head/neck for puncture. The inclination angle for puncture varies in different segments. The closer the segment is to the lower thoracic vertebrae, the larger the horizontal inclination angle of puncture is. This study also provides an anatomic reference for performing clinical intervertebral foramen puncture with ultrasound guidance.

Citation: Wang R, Sun WW, Han Y, Fan XX, Pan XQ, Wang SC, Lu LJ. Observation and measurement of applied anatomical features for thoracic intervertebral foramen puncture on computed tomography images. *World J Clin Cases* 2021; 9(18): 4607-4616

URL: <https://www.wjgnet.com/2307-8960/full/v9/i18/4607.htm>

DOI: <https://dx.doi.org/10.12998/wjcc.v9.i18.4607>

INTRODUCTION

Interventional therapy on the thoracic nerve roots or dorsal root ganglia (DRGs) is an important means to relieve chronic pain of the chest and abdomen, such as postherpetic neuralgia, incision pain, or other thoracic nerve pain[1-3]. The thoracic intervertebral foramina (TIVFs) are the most direct and frequently used channels for reaching the DRGs with interventional tools[4,5]. Therefore, accurate TIVF puncture is the key step for interventional treatment, which can determine the success or failure of total therapy. The anatomical features of the thoracic spine are complex. The presence of the transverse processes, ribs, and pleural and lung tissue increases the difficulty and risk of TIVF puncture[6,7]. Interventional procedures involving passage through the TIVFs have been performed for many years, and X-ray, computed tomography (CT), and ultrasound imaging have been used as common guidance solutions[5,7,8].

P-Reviewer: Watanabe K**S-Editor:** Zhang H**L-Editor:** Wang TQ**P-Editor:** Liu JH

However, few studies on the anatomy of the TIVFs have been reported, and even fewer literature reviews on the applied anatomy for TIVF cannulation have been published.

The thoracic spine is located between the cervical and lumbar vertebrae and includes the skeletal features of these vertebrae. However, the spatial relationship of the thoracic spine and the surrounding tissue is more complex than that of the cervical and lumbar segments. The anterior, superior, and inferior boundaries of the TIVFs consist of the corresponding vertebrae and their intervertebral discs, the inferior part of the pedicle, and the superior part of the pedicle. The posterior boundaries of the TIVFs consist of the articular processes of the zygapophyseal joint. Outside of the TIVFs are the thoracic paravertebral spaces and pleura on the lateral sides and the transverse processes on the superior lateral and inferior lateral sides. Inside of the TIVFs is the spinal cord[6]. The puncture trajectory usually passes from lateral to medial along the outer edge of the articular process. Therefore, the accessible space for TIVF cannulation is restricted to the intertransverse process space (ITPS). Additionally, the spinal nerves regularly exit the intervertebral foramina from the upper part, increasing the precision requirement of target positioning[4,9,10]. The available space for puncture adjustment is further restricted due to the presence of lung tissue and ribs, which is another difference from the anatomy of the cervical and lumbar spines. Although the spatial features of the TIVFs and surrounding structures are important for cannulation, the corresponding applied anatomy has not been sufficiently summarized. The difference in features between the upper, middle, and lower thoracic segments has also been vaguely described.

In TIVF puncture, the rib head and rib neck are the leading obstructions to achieving the desired trajectory. In this article, we summarize and report on the spatial relationship between the ribs and intertransverse spaces as well as the puncture characteristics for TIVF cannulation. This study may provide an important reference for image-guided TIVF puncture, especially using ultrasound imaging.

MATERIALS AND METHODS

Patients

This study was approved by the Ethics Committee of Nanjing Drum Tower Hospital Clinical College of Xuzhou Medical University (Ethical Number: 2020-347-01). A total of 88 patients who underwent thoracic minimally invasive treatment at Nanjing Drum Tower Hospital from January 2019 to June 2020 were admitted, including 41 males and 47 females, with an average age of 58.46 ± 10.12 years (range, 42-91 years). CT images of 167 segments of the thoracic intervertebral foramina were scanned and collected with the patients in the prone position during their operations. The inclusion criteria were as follows: (1) Minimally invasive surgery of the thoracic spinal nerve under CT guidance; (2) scanning of the TIVFs with slice thickness < 2 mm; and (3) scans obtained with patients in the prone position, cushioned with a pillow below the chest. Patients with the following criteria were excluded: (1) Spinal deformities, spinal bone lesions, or other diseases that affect normal thoracic anatomy; (2) a history of spinal surgery; (3) body mass index > 35 kg/m²; (4) severe skew in the scanning posture; and (5) severe osteoporosis. For the T1-2 to the T12-L1 TIVF segments, images were obtained from 6, 17, 23, 23, 14, 16, 12, 16, 16, 16, 10, 8, and 6 patients, respectively.

Measurement of spatial position parameters of the rib head/neck and transverse process spaces

CT data of the thoracic vertebrae in DICOM format were imported into Mimics software (materialize 17.0, Belgium), and three-dimensional skeletal structure models of the thoracic vertebrae were reconstructed. To improve the consistency of the characteristic measurements for different TIVF segments, the viewing angle was adjusted to the anteroposterior position. That is, when observed with the software in fluoroscopy mode, the spinous process line coincides with the middle line of the bilateral pedicle, and the anterior edge of the inferior border of the superior thoracic vertebra coincides with the posterior edge. Before measurement of each TIVF, the observation angle of the measured segment image was readjusted again. Then, the spatial position parameters of the rib head/neck and the transverse process space on both sides were measured (Figure 1).

Under this observation angle, the following parameters were measured: (1) The width of the intertransverse process space (D_p), that is, the vertical distance from the horizontal line of the inferior margin of the superior transverse process to the

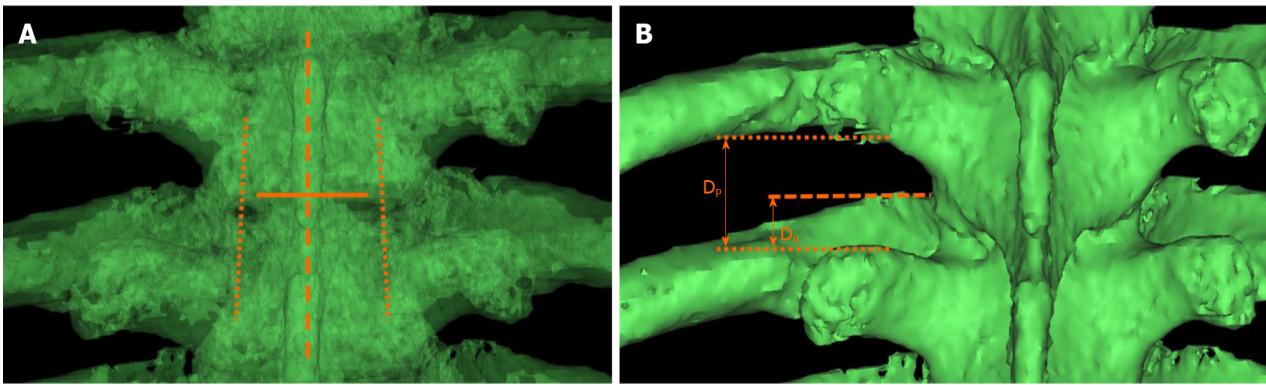


Figure 1 Measurement of spatial position parameters of the rib head/neck and transverse process space. A: Adjustment of the observation angle: The spinous process line (dashed) is located in the middle of the bilateral pedicle lines (dotted), and the inferior border coincides with the anteroposterior border (solid line) of the superior thoracic vertebra; B: Parameter measurement: The vertical distance from the horizontal line of the inferior margin of the superior transverse process to the horizontal line of the superior margin of the inferior transverse process (dotted) is the width of the transverse process space; the vertical distance from the horizontal line of the highest point of the rib neck/head (dashed) to the horizontal line of the superior margin of the inferior transverse process (dotted) is the height of the rib neck/head protrusion. D_p : The width of the intertransverse process space; D_R : The height of the rib neck/head protrusion.

horizontal line of the superior margin of the inferior transverse process; and (2) the height of the rib neck/head protrusion (D_R), that is, the vertical distance from the horizontal line of the highest point of the rib neck/head to the horizontal line of the superior margin of the inferior transverse process. The ratio D_R/D_p was used to assess the occlusion of the thoracic transverse process space by the rib head/neck. The value of D_R/D_p for each intervertebral foramen was calculated and trichotomized as $D_R/D_p = 0$, $0 < D_R/D_p \leq 1/2$, or $D_R/D_p > 1/2$. Then, the D_R/D_p values of the upper (T1-5), middle (T5-9), and lower (T9-L1) segments were compared.

Measurement of parameters related to TIVF puncture

The three-dimensional model of the thoracic vertebrae was sectioned with the reslice function of the software. The tomographic plane was placed parallel to the inferior border of the superior vertebral body, and the parameters were measured on the newly obtained tomographic plane. After positioning the tomographic image at the upper 1/3 level of the intervertebral foramen, the following parameters were measured: (1) The width of the lateral border of the articular process/lamina (W_p); (2) The width of the posterior border of the vertebral body (W_v); and (3) The horizontal inclination angle (α) from the lateral border of the articular process/lamina to the posterolateral border of the vertebral body (Figure 2). The ratio W_p/W_v was calculated to evaluate the changes in the vertebral body parameters of different segments. The inclination angles were compared between two sides. The correlation between inclination angle and segment location was also counted.

Statistical analysis

Statistical analyses were carried out using SPSS Version 22.0 (IBM Corporation, Armonk, NY, United States). The Shapiro-Wilk test was used to assess the normality of the distribution of the quantitative parameters. Quantitative data conforming to a normal distribution are described as the mean \pm SD, and comparisons were made by *t*-tests. Qualitative parameters are expressed as counts and percentages and were compared by the chi-square test. Pearson linear correlation analysis was used to describe the direction and degree of linear correlation between two quantitative variables. $P < 0.05$ was considered statistically significant.

RESULTS

Spatial relationship of the rib head/neck and ITPS

The height of the rib neck/head protruding into the ITPS differed in different thoracic vertebral segments, resulting in different degrees of occlusion (Figure 3). No rib head/neck occlusion ($D_R/D_p > 0$) onto the ITPS was found on segments T1-2 and T12-L1, and the remaining thoracic segments were all occluded by the rib. The details of ITPS obstruction by the rib head/neck from T1-2 to T12-L1 are shown in Table 1. The

Table 1 Occlusion of the transverse process spaces of different segments by the rib head/neck (both sides)

Segment	No occlusion	0 < Occlusion ≤ 1/2	Occlusion > 1/2
T1-2 (<i>n</i> = 12)	12 (100%)	0	0
T2-3 (<i>n</i> = 34)	15 (44.12%)	19 (55.88%)	0
T3-4 (<i>n</i> = 46)	5 (10.87%)	39 (84.78%)	2 (4.35%)
T4-5 (<i>n</i> = 46)	0	37 (80.43%)	9 (19.57%)
T5-6 (<i>n</i> = 28)	0	15 (53.57%)	13 (46.43%)
T6-7 (<i>n</i> = 32)	0	4 (12.50%)	28 (87.50%)
T7-8 (<i>n</i> = 24)	0	5 (20.83%)	19 (79.17%)
T8-9 (<i>n</i> = 32)	0	6 (18.75%)	26 (81.25%)
T9-10 (<i>n</i> = 32)	0	10 (31.25%)	22 (68.75%)
T10-11 (<i>n</i> = 20)	0	16 (80.00%)	4 (20.00%)
T11-12 (<i>n</i> = 16)	2 (12.50%)	14 (87.50%)	0
T12-L1 (<i>n</i> = 12)	12 (100%)	0	0

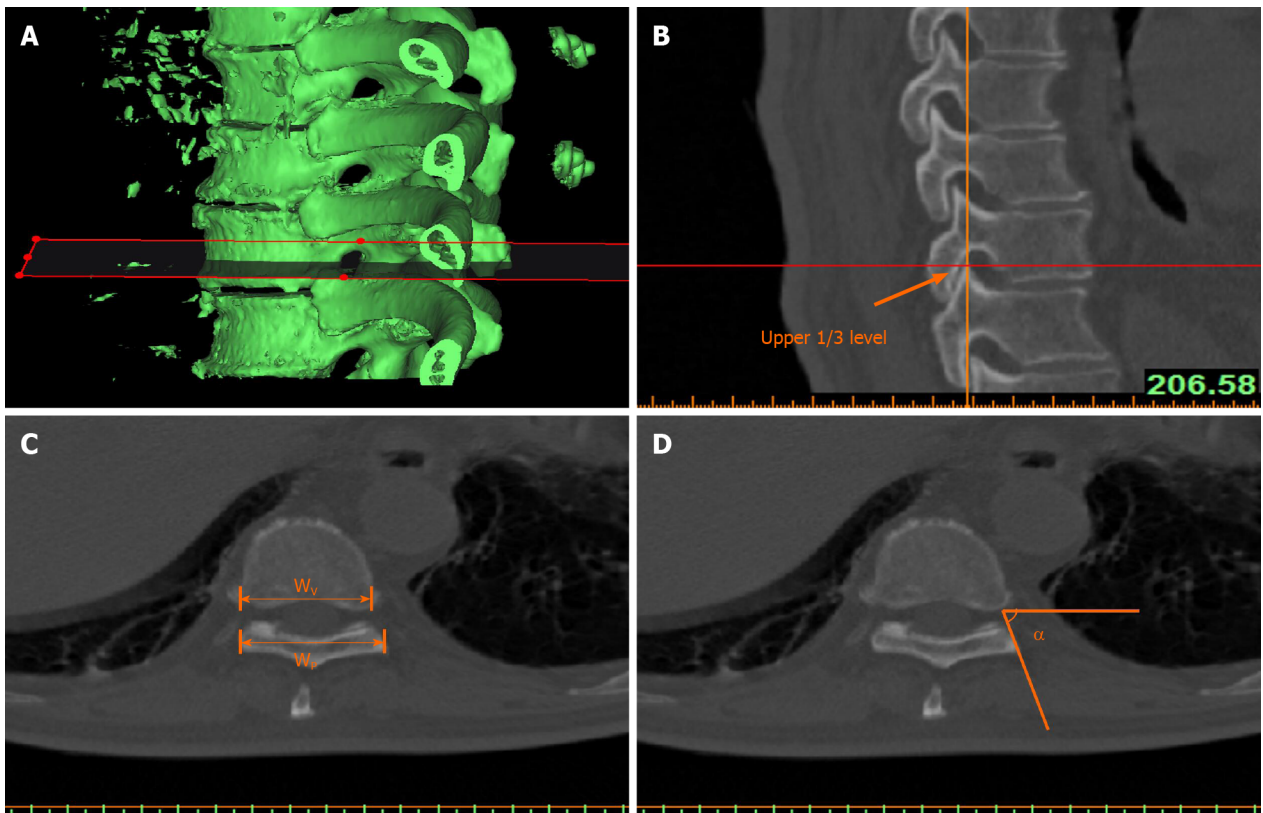


Figure 2 Measurement of parameters related to the intervertebral foramen. A and B: The three-dimensional model of the thoracic vertebra was resliced parallel to the inferior border of the superior vertebral body of the intervertebral foramen, and the upper 1/3 level tomographic image of the intervertebral foramen was selected for parameter measurement; C and D: The width of the lateral border of the articular process/lamina; the width of the posterior border of the vertebral body; and the horizontal inclination angle from the lateral border of the articular process/lamina to the posterolateral border of the vertebral body. W_p : The width of the lateral border of the articular process/lamina; W_v : The width of the posterior border of the vertebral body; α : The horizontal inclination angle from the lateral border of the articular process/lamina to the posterolateral border of the vertebral body.

incidence of occlusion for the upper thoracic segments (T1-5, *n* = 138), middle thoracic segments (T5-9, *n* = 116), and lower thoracic segments (T9-L1, *n* = 80) was 76.81%, 100%, and 82.50%, respectively. The incidence of occlusion for the middle thoracic segments was significantly higher than that for the upper and lower thoracic segments ($P < 0.05$). The incidence of $> 1/2$ occlusion ($D_R/D_P > 1/2$) of the ITPS for the upper, middle, and lower thoracic segments was 7.97%, 74.14% and 32.50%, respectively. The

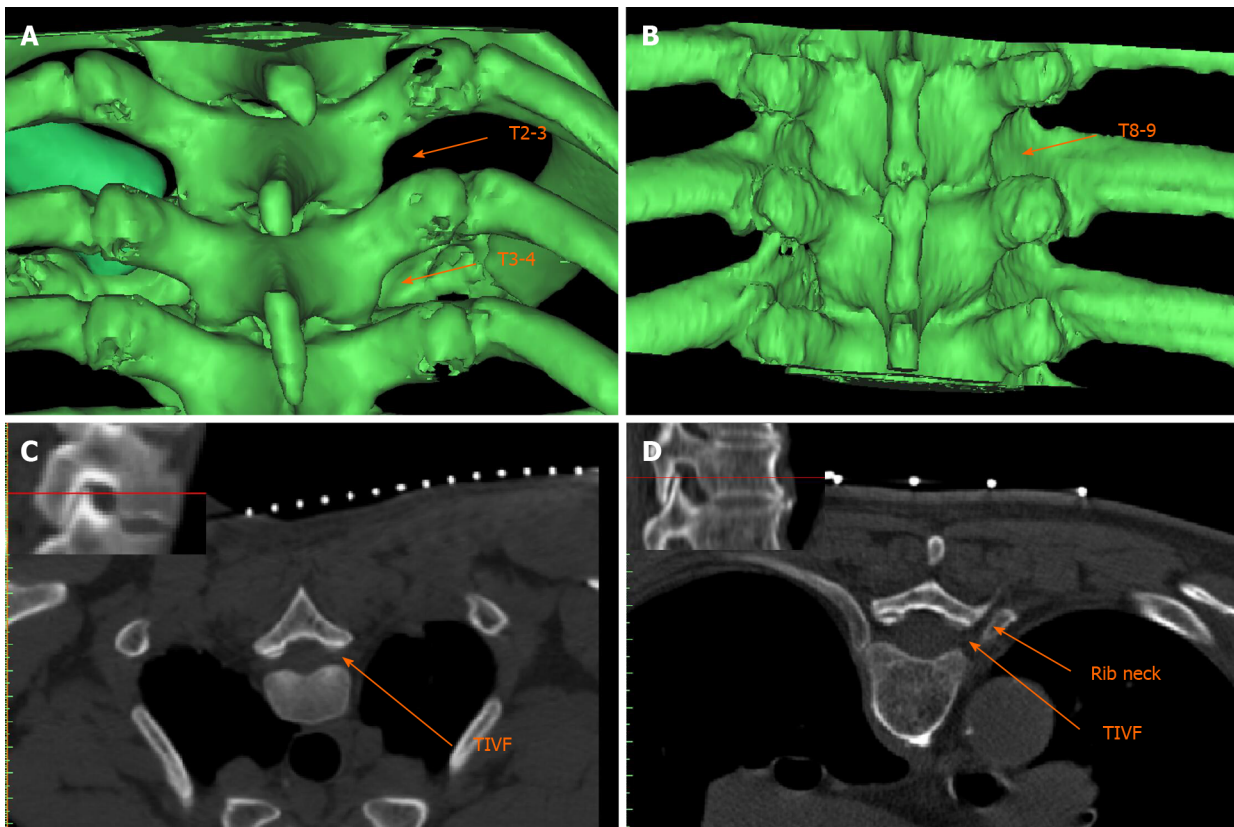


Figure 3 Spatial position of the rib head/neck and transverse process space. A and B: The T2-3 intertransverse process space (ITPS) is not occluded by the rib neck/head, while the T3-4 ITPS is partially occluded, and the T8-9 ITPS is completely covered; C: The upper 1/3 level tomographic image of the T2-3 intervertebral foramen shows no occlusion by the corresponding rib neck/head; D: The upper 1/3 level tomographic image of the T8-9 intervertebral foramen shows occlusion by the corresponding rib neck; puncture of the intervertebral foramen would need to pass through the gap between the vertebral plate and the rib neck. TIVF: Thoracic intervertebral foramen.

incidence of $> 1/2$ ITPS occlusion for the middle thoracic segments was significantly higher than that for the upper and lower thoracic segments ($P < 0.05$) (Table 2).

Puncture parameters at the upper 1/3 level of the TIVFs

At the upper 1/3 level of the intervertebral foramina, the width of the lateral border of the articular process/lamina (W_p) was longer than the width of the posterior border of the vertebral body (W_v) for segments T1-2 to T9-10. W_p started to be shorter than W_v from segment T10-11 to segment T12-L1 (Table 3). No significant difference in the horizontal puncture angle (α) was found between the left and right sides. The horizontal puncture angle (α) into the external opening of the intervertebral foramina was positively correlated with the thoracic vertebral segments from the cephalic to caudal portion (left: $r = 0.772$, $P < 0.01$; right: $r = 0.771$, $P < 0.01$). On the T11-12 and T12-L1 segments, the horizontal inclination angle was 90° , and a perpendicular puncture close to the lateral border of the lamina/articular process entered the external opening of the intervertebral foramina.

DISCUSSION

Accurate TIVF puncture can reduce operation risks and complications of interventional treatment[11]. By measuring the relevant parameters of thoracic intervertebral foramen puncture on three-dimensional reconstructed CT images, the purpose of this study was to observe the spatial, applied anatomical characteristics of different thoracic intervertebral foramen segments. We also sought to provide an anatomical basis for clinical puncture operations, especially in the application of ultrasound-guided thoracic intervertebral foramen puncture.

The thoracic intervertebral foramina are important channels for the minimally invasive interventional treatment on the thoracic nerve roots and dorsal root ganglia in the field of pain management[4]. Accurate localization and puncture of the TIVFs are

Table 2 Occlusion of the transverse process spaces of upper, middle, and lower segments by the rib head/neck (both sides)

Segment	Occlusion	Occlusion > 1/2
Upper segments (T1-5, <i>n</i> = 138)	106 (76.81%) ^a	11 (7.97%) ^a
Middle segments (T5-9, <i>n</i> = 116)	116 (100%)	86 (74.14%)
Lower segments (T9-L1, <i>n</i> = 80)	66 (82.5%) ^a	26 (32.50%) ^a

^a*P* < 0.05 vs middle segments.

Table 3 Parameters related to the upper 1/3 level of the intervertebral foramen for puncture

Segment	Wp/Wv > 1	Wp/Wv ≤ 1	Puncture angle (left)	Puncture angle (right)	<i>P</i> value
T1-2 (<i>n</i> = 6)	6 (100%)	0	42.73 ± 2.73	48.95 ± 2.20	0.151
T2-3 (<i>n</i> = 17)	17 (100%)	0	62.55 ± 8.51	61.76 ± 6.71	0.484
T3-4 (<i>n</i> = 23)	23 (100%)	0	69.02 ± 5.76	69.68 ± 6.09	0.705
T4-5 (<i>n</i> = 23)	23 (100%)	0	71.76 ± 4.89	71.93 ± 6.67	0.925
T5-6 (<i>n</i> = 14)	14 (100%)	0	71.10 ± 6.13	70.88 ± 7.00	0.709
T6-7 (<i>n</i> = 16)	16 (100%)	0	73.78 ± 3.39	73.68 ± 4.53	0.944
T7-8 (<i>n</i> = 12)	12 (100%)	0	76.96 ± 4.96	75.91 ± 4.22	0.581
T8-9 (<i>n</i> = 16)	16 (100%)	0	79.26 ± 5.25	79.74 ± 5.65	0.805
T9-10 (<i>n</i> = 16)	16 (100%)	0	76.65 ± 4.98	77.12 ± 5.72	0.808
T10-11 (<i>n</i> = 10)	7 (70%)	3 (30%)	83.29 ± 6.92	82.98 ± 6.53	0.918
T11-12 (<i>n</i> = 8)	0	8 (100%)	90 ± 0	90 ± 0	-
T12-L1 (<i>n</i> = 6)	0	6 (100%)	90 ± 0	90 ± 0	-

P value: Comparison of puncture angle between the right and left. W_p: The width of the lateral border of the articular process/lamina; W_v: The width of the posterior border of the vertebral body.

the basis for successful treatment[11]. Currently, thoracic intervertebral foramen puncture is usually performed under the guidance of C-arm or CT. X-rays can show the relationship between bony structures and the puncture needle. Three-dimensional reconstructed CT images can not only show the 3D spatial relationship between the structures adjacent to the TIVF but also provide a reference for operation planning and puncture path optimization[4,12,13]. However, C-arm and CT guidance also have some disadvantages, such as radiation exposure to the operators and patients, poor portability, and inability to guide in real time.

The thoracic intervertebral foramina are the bony channels where the thoracic nerve roots leave the spinal cord. The structure of the thoracic intervertebral foramina is significantly different from that of the cervical and lumbar segments, which is mainly manifested by rib head/neck occlusion. Our results showed that only the T1-2 and T12-L1 segments lacked rib occlusion in the ITPS. The ITPSs of the other segments were all occluded by the rib head/neck. The middle thoracic segments had the highest incidence of occlusion, and their incidence of > 1/2 occlusion was significantly higher than that of the upper thoracic and lower thoracic segments.

At the upper 1/3 level of the intervertebral foramina, the width of the lateral border of the articular process/lamina of the T1-10 segments was longer than the width of the posterior border of the vertebral body, which indicates that the puncture needle needs to pass through the lateral margin of the lamina at a certain angle to enter the intervertebral foramen. From the cephalic to caudal portion, the horizontal inclination angle required to enter the external opening of the intervertebral foramen gradually increases. Therefore, on the upper thoracic segments, especially the T1-2 segment, sufficient lateral distance is required to enter the intervertebral foramen. On the middle thoracic segments, the lateral distance is smaller than that on the upper thoracic segments. However, because the rib head/neck occupies the ITPS, it is necessary to design the trajectory along the tangent line of the rib head/neck and

lamina so that the needle can smoothly pass through the gap and enter the intervertebral foramen. On the lower thoracic segments, the width of the lateral border of the lamina/facet joint becomes increasingly shorter than that of the posterior border of the vertebral body. Therefore, excessive lateral distance should be avoided due to the risk of puncture into the spinal canal, which can lead to spinal cord injury and other serious complications.

In recent years, ultrasound has been increasingly used in minimally invasive interventional treatment of the spine[14,15]. However, because ultrasound cannot penetrate bone, the location of spinal targets often relies on the surface anatomical characteristics of bony structures[6,16]. The 12 segments of the thoracic vertebrae are located between the cervical and lumbar vertebral segments. The upper and lower thoracic spines possess characteristics of the cervical and lumbar spines, respectively. However, the paravertebral structure of the thoracic vertebrae is more complex, and the application of ultrasound-guided TIVF puncture is highly risky[11]. This study summarized the spatial features of the skeletal structure and provides a reference for ultrasonic TIVF puncture.

In the process of ultrasound-guided TIVF puncture, the short axis section of the transverse process should be assessed first. Then, the probe should be moved to the caudal side until the transverse process disappears, where the ITPS section can be obtained. Generally, the main structure of the ITPS section includes the lamina/articular process, paravertebral space, and pleura[17,18]. In this section, the intervertebral foramen is the space formed by the superficial lamina/facet joint and the posterior margin of the deep vertebral body. Adopting the in-plane technique, the TIVF can be entered along the lateral border of the lamina/articular process. However, based on the results of this study, we found that not only the pleura is found outside the TIVF in the ITPS section but also a hyperechoic rib head/neck may occupy the external area of the TIVF and occlude the puncture path (Figure 3C and D), especially in the middle thoracic segments. After moving the probe caudally until the transverse process echo disappears, combined ultrasonic images of the vertebral plate/articular process, rib head/neck, and pleura appear. Since the space between the rib head/neck and lamina/articular process is not a joint structure, we propose that this gap should be a feasible puncture path into the intervertebral foramen in this plane.

CONCLUSION

In summary, the anatomical structure of the thoracic intervertebral foramen is unique. The rib head/neck in the middle thoracic segments greatly influences the puncture path for the intervertebral foramen; therefore, it is necessary to identify the space between the transverse process and rib head/neck for puncture. The inclination angle for puncture differs in different segments. The closer the segment is to the lower thoracic vertebrae, the larger the horizontal inclination angle of puncture is. This study also provides an anatomic reference for performing clinical intervertebral foramen puncture with ultrasound guidance.

ARTICLE HIGHLIGHTS

Research background

When conducting interventional therapy on the thoracic nerve roots or dorsal root ganglia for treatment of chronic pain, thoracic intervertebral foramen (TIVF) is the most frequently used channel and TIVF puncture is the key step for the therapy. The anatomical features of the structure around TIVF are complex. Despite the assistance of many imaging guidance, clinical application of TIVF cannulation is still challenging. Improper operation may injure the pleura, blood vessels, spinal cord, and other tissues, causing serious complications.

Research motivation

The intertransverse process space (ITPS) for TIVF cannulation is severely restricted by the lung and ribs, but the spatial anatomical characteristics and related parameters for TIVF puncture remain poorly understood. The difference in features between the upper, middle, and lower thoracic segments has also been vaguely described.

Research objectives

To observe and summarize the spatially applied anatomical characteristics for TIVF puncture on different vertebral segments.

Research methods

A total of 88 patients who underwent thoracic minimally invasive interventional treatment were included. Computed tomography images of 167 thoracic vertebral segments scanned in the prone position were collected. We measured the width of the ITPS (D_p), the height of the rib neck/head above the lower transverse process (D_r), the width of the lateral border of the articular process/lamina (W_p), and the width of the posterior border of the vertebral body (W_v). The horizontal inclination angle (α) for TIVF puncture at the upper 1/3 level of the intervertebral foramina was measured. The above measured parameters and calculated ratios (D_r/D_p and W_p/W_v) were compared between segments.

Research results

No rib head/neck occlusion ($D_r/D_p > 0$) was found in the ITPS of T1-2 and T12-L1. The incidence of occlusion for the middle thoracic segments was significantly higher than that for the upper and lower thoracic segments. The incidence of $> 1/2$ occlusion for the middle thoracic segments was significantly higher than that for the upper and lower thoracic segments. W_p was longer than W_v on T1-2 to T9-10 and shorter than W_v on T10-11 to T12-L1. The horizontal puncture angle (α) into the external opening of the TIVF was positively correlated with the segments of the thoracic vertebrae from the cephalic to caudal portion.

Research conclusions

The impact of the rib head/neck on the puncture path of the TIVF varies on different segments. It is necessary to identify spatial structure and design appropriate puncture angles for different segments.

Research perspectives

In this article, we summarize and report on the spatial relationship between the ribs and ITPS as well as the puncture characteristics for thoracic intervertebral foramina cannulation. This study also provides an anatomic reference for performing clinical intervertebral foramen puncture, especially with ultrasound guidance.

REFERENCES

- 1 **Han Z**, Hong T, Ding Y, Wang S, Yao P. CT-Guided Pulsed Radiofrequency at Different Voltages in the Treatment of Postherpetic Neuralgia. *Front Neurosci* 2020; **14**: 579486 [PMID: 33390880 DOI: 10.3389/fnins.2020.579486]
- 2 **Makharita MY**, Amr YM. Effect of Repeated Paravertebral Injections with Local Anesthetics and Steroids on Prevention of Post-herpetic Neuralgia. *Pain Physician* 2020; **23**: 565-572 [PMID: 33185373]
- 3 **Cohen SP**, Sireci A, Wu CL, Larkin TM, Williams KA, Hurley RW. Pulsed radiofrequency of the dorsal root ganglia is superior to pharmacotherapy or pulsed radiofrequency of the intercostal nerves in the treatment of chronic postsurgical thoracic pain. *Pain Physician* 2006; **9**: 227-235 [PMID: 16886031]
- 4 **Zhu J**, Fei Y, Deng J, Huang B, Yao M. Application and Therapeutic Effect of Puncturing of the Costal Transverse Process for Pulsed Radiofrequency Treated T1-T3 Herpes Zoster Neuralgia. *J Pain Res* 2020; **13**: 2519-2527 [PMID: 33116793 DOI: 10.2147/JPR.S266481]
- 5 **Lee HJ**, Park HS, Moon HI, Yoon SY. Effect of Ultrasound-Guided Intercostal Nerve Block Versus Fluoroscopy-Guided Epidural Nerve Block in Patients With Thoracic Herpes Zoster: A Comparative Study. *J Ultrasound Med* 2019; **38**: 725-731 [PMID: 30244489 DOI: 10.1002/jum.14758]
- 6 **Krediet AC**, Moayeri N, van Geffen GJ, Bruhn J, Renes S, Bigeleisen PE, Groen GJ. Different Approaches to Ultrasound-guided Thoracic Paravertebral Block: An Illustrated Review. *Anesthesiology* 2015; **123**: 459-474 [PMID: 26083767 DOI: 10.1097/ALN.0000000000000747]
- 7 **Ding Y**, Li H, Hong T, Zhao R, Yao P, Zhao G. Efficacy and Safety of Computed Tomography-Guided Pulsed Radiofrequency Modulation of Thoracic Dorsal Root Ganglion on Herpes Zoster Neuralgia. *Neuromodulation* 2019; **22**: 108-114 [PMID: 30288853 DOI: 10.1111/ner.12858]
- 8 **Zhao P**, Mei L, Wang W. Clinical Study of Ultrasound-Guided Methylene Blue Thoracic Paravertebral Nerve Block for the Treatment of Postherpetic Neuralgia. *Turk Neurosurg* 2019; **29**: 811-815 [PMID: 31049917 DOI: 10.5137/1019-5149.JTN.24950-18.2]
- 9 **Hetta DF**, Mohamed SAB, Mohamed KH, Mahmoud TAE, Eltyb HA. Pulsed Radiofrequency on Thoracic Dorsal Root Ganglion Versus Thoracic Paravertebral Nerve for Chronic Postmastectomy

- Pain, A Randomized Trial: 6-Month Results. *Pain Physician* 2020; **23**: 23-35 [PMID: 32013276]
- 10 **Kim WJ**, Park HS, Park MK. The effect of needle tip position on the analgesic efficacy of pulsed radiofrequency treatment in patients with chronic lumbar radicular pain: a retrospective observational study. *Korean J Pain* 2019; **32**: 280-285 [PMID: 31569920 DOI: 10.3344/kjp.2019.32.4.280]
- 11 **Taketa Y**, Fujitani T. Approach affects injectate spread in ultrasound-guided thoracic paravertebral block: a cadaveric trial. *Br J Anaesth* 2017; **119**: 339-340 [PMID: 28854556 DOI: 10.1093/bja/aex209]
- 12 **Oertel MF**, Hobart J, Stein M, Schreiber V, Scharbrodt W. Clinical and methodological precision of spinal navigation assisted by 3D intraoperative O-arm radiographic imaging. *J Neurosurg Spine* 2011; **14**: 532-536 [PMID: 21275555 DOI: 10.3171/2010.10.SPINE091032]
- 13 **Luo C**, Yang B, Yang LQ, Wu BS, Wang XP, He LL, Zhao R, Ni JX, Tang YZ. Computed Tomography-Guided Percutaneous Coblation of the Thoracic Nerve Root for Treatment of Postherpetic Neuralgia. *Pain Physician* 2020; **23**: E487-E496 [PMID: 32967399]
- 14 **Patel A**, Kumar V, Garg R, Bhatnagar S, Mishra S, Gupta N, Bharti SJ, Kumar S. Comparison of analgesic efficacy of ultrasound-guided thoracic paravertebral block versus surgeon-guided serratus anterior plane block for acute postoperative pain in patients undergoing thoracotomy for lung surgery- A prospective randomized study. *Saudi J Anaesth* 2020; **14**: 423-430 [PMID: 33447181 DOI: 10.4103/sja.SJA_143_20]
- 15 **Ji K**, Wang Z, Zheng X, Wei H, Shi Y, Qian P. Application of ultrasound-guided paravertebral nerve block in preemptive analgesia of thoracic surgery. *Panminerva Med* 2020 [PMID: 33307641 DOI: 10.23736/S0031-0808.20.04215-9]
- 16 **Chang KV**, Wu WT, Özçakar L. Ultrasound-Guided Interventions of the Cervical Spine and Nerves. *Phys Med Rehabil Clin N Am* 2018; **29**: 93-103 [PMID: 29173667 DOI: 10.1016/j.pmr.2017.08.008]
- 17 **Luyet C**, Eichenberger U, Greif R, Vogt A, Szücs Farkas Z, Moriggl B. Ultrasound-guided paravertebral puncture and placement of catheters in human cadavers: an imaging study. *Br J Anaesth* 2009; **102**: 534-539 [PMID: 19244265 DOI: 10.1093/bja/aep015]
- 18 **Luyet C**, Siegenthaler A, Szucs-Farkas Z, Hummel G, Eichenberger U, Vogt A. The location of paravertebral catheters placed using the landmark technique. *Anaesthesia* 2012; **67**: 1321-1326 [PMID: 23130724 DOI: 10.1111/j.1365-2044.2012.07234.x]



Published by **Baishideng Publishing Group Inc**
7041 Koll Center Parkway, Suite 160, Pleasanton, CA 94566, USA
Telephone: +1-925-3991568
E-mail: bpgoffice@wjgnet.com
Help Desk: <https://www.f6publishing.com/helpdesk>
<https://www.wjgnet.com>

